Chinese Chemical Letters 32 (2021) 3382–3386

Contents lists available at ScienceDirect

Chinese Chemical Letters

journal homepage: www.elsevier.com/locate/cclet

Communication

Renewable molybdate complexes encapsulated in anion exchange resin for selective and durable removal of phosphate

Wei Zhu, Xiaohua Huang, Yi Zhang, Zhonglong Yin, Zhen Yang*, Weiben Yang*

School of Chemistry and Materials Science, Jiangsu Provincial Key Laboratory of Materials Cycling and Pollution Control, Nanjing Normal University, Nanjing 210046, China

ARTICLE INFO

Article history:
Received 11 January 2021
Revised 15 February 2021
Accepted 16 April 2021
Available online 22 April 2021

Keywords:
Molybdate composite adsorbent
Resin
Phosphate removal
Selective and durable adsorption
Structural transformation of complexes

ABSTRACT

The existence of many anions in wastewater reduces the removal efficiency of phosphate by adsorbents under realistic conditions. Facing this challenge, the study reports on an insistent and stable composite adsorbent of molybdate complexes Fe-(MoO_x) embedded in a macroporous anion exchange resin (D-201). [Fe(MoO_x)]-D-201 shows 93.7% adsorption capacity (28.3 mg/g) for phosphate even when the molar concentration of coexisting ions is 5 times higher than phosphate. The capacity of adsorbent is maintained more than 84.2% after five regeneration cycles to remove phosphate in the wastewater containing coexisting ions. The ability of highly selective removal of phosphate is maintained during the regeneration cycles explained by the change of the binding of molybdate clusters with phosphate, which is due to the different structures of molybdate clusters depending on various pH. In general, this work puts forward a new idea for the development of phosphorus removal adsorbents for the treatment of wastewater containing coexisting ions.

Phosphorus (P) is an essential nutrient for plant growth, but its excessive phosphorous release into run-off from human activities is considered as one major cause of eutrophication, which imposes great risk to the ecosystem [1–3]. Until now, numerous methods have been developed for phosphorus removal from contaminated waters [4,5]. The adsorption technique is regarded as the most promising approach because of its simplicity, effective-ness and relatively low-cost [6–8]. A wide range of inorganic pollutants (*e.g.*, SO_4^{2-}, NO_3^- or HCO_3^-) are usually present in the water at much higher levels than phosphate, the preference and capacity of the concerned adsorbent is great importance to its feasibility in the real application [9,10]. Nowadays, many kinds of new generation adsorbents have been developed for selective phosphate removal, such as metal oxide-based composite adsorbent because they exhibit strong ligand sorption through the formation of inner-sphere complexes *via* Lewis acid-base interactions [11–14]. But under the same condition, various coexisting anions are easily adsorbed onto adsorbents. So, the adsorption selectivity of the material decreased a lot. To tackle this problem, it necessitates the development of phosphate adsorbents with high selectivity.

The reaction between molybdate and phosphate is often used to detect trace phosphorus in water [15,16]. Therefore, molybdate materials are expected to exhibit good adsorption and selective separation towards phosphate. As for the practical application of molybdate complexes, their poor mechanic strength greatly limits the prolonged use in water treatment. The molybdate complex particles inside solid hosts of large-sized porous structure with better mechanical strength is an effective approach to overcome the above technical challenge. Though numerous hosts have been reported for this purpose [17,18], polymeric exchanger of crosslinking structure is one of the most promising choices because of its durability [19,20], reliable mechanic strength, and sufficient pore spaces to accommodate and disperse molybdate complex particles, such as the famous commercial anion exchanger D-201 [21,22]. In recent reports, the macroporous strong base anion exchange resin D-201 with polystyrene matrix and quaternary amine functional groups, have been successfully used for the host of various composite adsorbents. Besides, quaternary amine groups on D-201 backbones provide loaded sites for anionic molybdate clusters. The covalently bound positively charged groups of D-201 favour the dispersion of molybdate complex particles as well as sorption enhancement of the anionic pollutants based on Donnan principle [23–25].

Relevant literature has been reported a new method of loading polyoxometalates on resins for the removal of phosphate [26], it

* Corresponding authors.
E-mail addresses: yangzhen@njnu.edu.cn (Z. Yang), yangwb007@njnu.edu.cn (W. Yang).

https://doi.org/10.1016/j.cclet.2021.04.027
1001-8417/

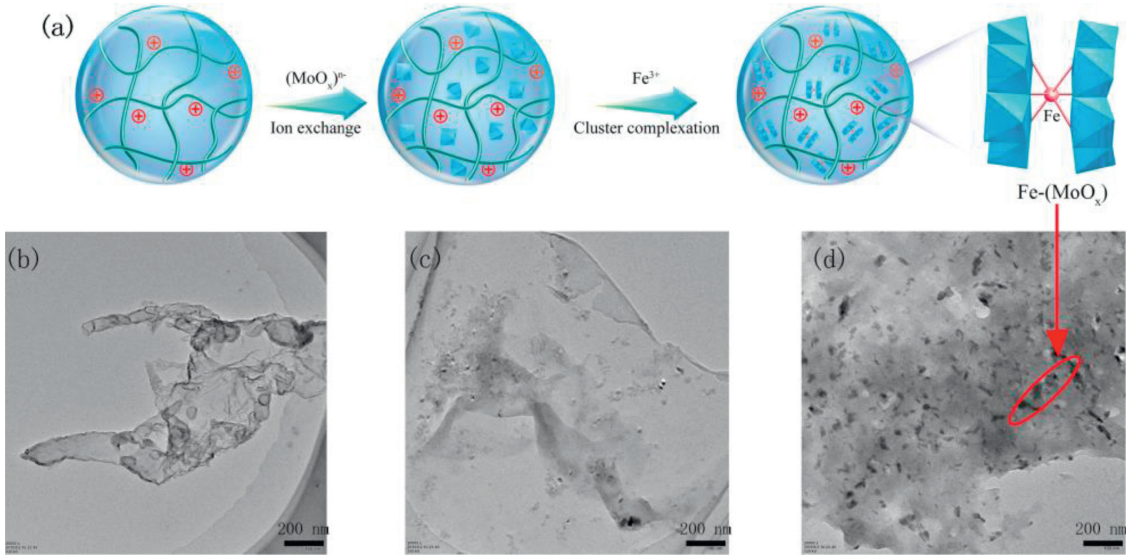

Fig. 1. (a) Synthetic method of FM-201. (b-d) TEM images of (b) original D-201, (c) M-201 and (d) FM-201.

inspired us to create the new molybdate composite adsorbent for highly efficient phosphate removal from wastewater. We proposed a new idea that pH can be controlled to change the binding ability of molybdate complexes toward phosphate *via* MoO_x structural transformation, and studied the change of molecular behaviour of materials in the process of adsorption-regeneration. In this study, we report the very valuable finding that molybdate-composite adsorbent FM-201 maintain its selective phosphorus removal ability after acid solution regeneration.

Reactant chemical sources and purities are described in Section S1 (Supporting information). Here, we employed D-201 as the host for the molybdate complexes. According to the synthesis method in Fig. 1a, [Fe(MoO_x)]-D-201 (FM-201) is prepared (Section S2 in Supporting information). Another similar composite adsorbent [Zr(MoO_x)]-D-201 (ZM-201)) is also synthesized with $ZrOCl_2 \cdot 8H_2O$ as a comparison. The detailed material characterization for FM-201 are provided in Table S1 and Fig. S1 (Supporting information). The experimental procedures for the kinetic, effect of pH, isotherm, effect of coexisting competitive ions, regeneration tests and fixed-bed column experiments are in Sections S4-S7 (Supporting information).

TEM images (Figs. 1b–d) indicate the changes of surface morphology of resin during synthesis of FM-201. As shown in the Fig. S2 (Supporting information), Fe-(MoO_x) particles with different sizes are loaded on the inner and outer surface of D-201, whereas the pristine D-201 has a relatively smooth surface. Before the formation of complexes with Fe^{3+}, the molybdate particles on the surface of D-201 are very small. The particles of Fe-molybdate complexes on the surface of D-201 is beneficial for the stability of FM-201.

The FT-IR spectras of the new adsorbents compared to the pristine resin show the characteristic peaks of the molybdate complexes embedded in the resin (Fig. S1a). The peaks at 912, 914 and 947 cm^{-1}, indicate the presence of the molybdate group (Mo = O). Similarly, the peaks at 833 and 845 cm^{-1} indicate the presence of metal coordination bonds (Mo-O-Fe and Mo-O-Zr) [27]. Additionally, the FT-IR spectras of the adsorbents is distinguishable from the pristine resin by the peaks in the range of 409–523 cm^{-1} and 413–523 cm^{-1}, indicating the stretching vibration of the metal-oxygen (Fe-O, Zr-O). By comparison with the Raman spectras of D-201 (Fig. S1b), those of the prepared adsorbent suggest the presence of a molybdena species to the MoO_x clusters because of the presence of Mo=O stretching modes (940 and 991 cm^{-1} in FM-201; 963 and 991 cm^{-1} in ZM-201). In addition, the Raman bands from 200 to 370 cm^{-1} reflect bending mode of the bridging Mo-O-Mo bonds. The physiochemical properties and characterization results of adsorbents are summarized in Table S1. The BET surface area increased from 15.93 m^2/g of the host D-201 to 23.73 m^2/g of FM-201, while its average pore diameter decreased from 26.47 to 18.74 nm as a result of pore blockage caused by the loaded Fe-(MoO_x) complexes. The higher specific surface area compared to D-201 is presumed to be favourable for adsorption. The loading amount of Mo in FM-201 is 15.74 wt%, it is larger than 13.67 wt% in ZM-201 although the content of Fe in the FM-201 is lower than Zr in ZM-201.

As the adsorbent, its stability in water is important. Molybdenum leaching from the materials at different pHs is then measured (Fig. S3 in Supporting information), as it determines the performance and reusability of the adsorbents. Mo in M-201 is easy to escape, while FM-201 and ZM-201 remain stable with Mo loss less than 1 wt% when pH is less than 7. Therefore, the complexation of Fe^{3+} and Zr^{2+} improve the stability of molybdate adsorbents.

Effects of pH on the adsorption performance are investigated at first, the adsorbents have pH-responsiveness because of the existence of quaternary ammonium and molybdate. The adsorption ability of different adsorbents for the removal of phosphate from water is evaluated in a wide pH range. As shown in Fig. 2a, the phosphate adsorption capacity appears to be quite dependent upon the pH. The composite adsorbents exhibit the highest adsorption capacities at pH 5. The order of maximum adsorption capacities is FM-201 (30.2 mg/g) > ZM-201 (26.1 mg/g) > M-201 (21.7 mg/g) > D-201 (17.8 mg/g). Compared with M-201, adsorbents loaded with other metals (Fe or Zr) possessed significant better performance. Moreover, with more Mo contents, FM-201 has higher adsorption capacity than ZM-201. The concentration of phosphorus in natural sewage is generally lower than 10 mg/L, the maximum removal rate of phosphate is 97.6% by FM-201 in 10 mg P/L solution (Fig. S4 in Supporting information).

The kinetics of phosphate adsorption is important in assessing the adsorbent's performance. Fig. S5 (Supporting information) shows the adsorption kinetics of phosphate on FM-201. *Pseudo*-second-order kinetic model better fits the kinetic data (Table S2 in Supporting information), it reveals chemisorption between adsorbents and adsorbates, which is in accordance with previous deduc-

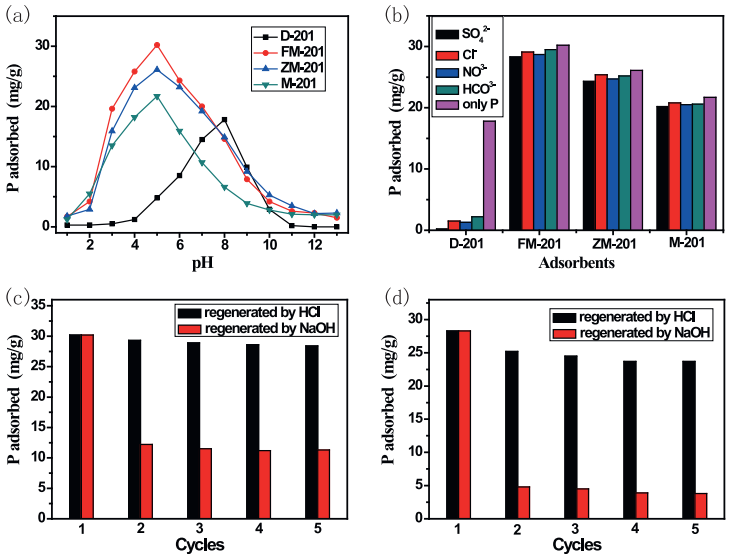

Fig. 2. (a) Effect of pH on phosphate uptake (adsorbent dose: 0.5 g/L; initial phosphate concentration: 30 mg/L; 25 °C; 24 h). (b) Effect of competitive anions on phosphate uptake (adsorbent dose: 0.5 g/L; initial phosphate concentration: 30 mg P/L; 25 °C; 24 h; coexisting anion concentration: 150 mg/L); Reusability of the FM-201 in 5 consecutive adsorption-regeneration cycles in (c) solution without coexisting ions (Initial phosphate concentration: 30 mg P/L; pH 5; adsorbent dosage: 0.5 g/L; regeneration solution: 2 mL of HCl (0.1 mol/L) or NaOH (0.1 mol/L); regeneration time: 2 h) and (d) with coexisting competitive SO_4^{2-} concentration: 150 mg/L.

tion that complexing actions between the phosphate and molybdate clusters. Another critical parameter for evaluating the performance of an adsorbent is the isotherms. The adsorption behaviour is well fitted by Langmuir isotherm models (Fig. S6 and Table S3 in Supporting information), indicating a monolayer coverage of phosphate adsorbed onto FM-201. We suggest that q_{max} is originated from the molybdate complexes, which is close to the experimental results and evidenced the specific interaction of molybdate complexes toward phosphate anions [28].

The structure of the composite adsorbents possess two distinct sites for phosphate adsorption, including the host ammonium groups and the clusters of molybdate, which are interacted with phosphate through the following equations Eqs. 1 and 2, respectively:

$$nR-(CH_3)_3+H_mPO_4^{(3-m)-}\rightarrow[R-(CH_3)_3]_n\left[H_mPO_4^{(3-m)-}\right] \quad (1)$$

$$H_mPO_4^{(3-m)-}+12MoO_x^{(2x-6)-}\rightarrow[PO_4\cdot MO_x]^{3-} \quad (2)$$

Effect of widely detected anions in water environment, such as SO_4^{2-}, Cl^-, NO_3^- and HCO_3^-, on phosphate adsorption are tested (Fig. 2b). Adsorption capacity of D-201 sharply decreased with the increasing concentration of competing anions. By contrast, FM-201 maintained 93.7% adsorption capacity even when the molar concentration of SO_4^{2-}, Cl^-, NO_3^- or HCO_3^- is 5 times higher than phosphate. Such results demonstrate the excellent adsorption selectivity of FM-201 towards phosphate. While ammonium groups of D-201 have no selectivity because they are interacted with anions through Coulomb force [29], the results show that the loading of molybdate generated selective adsorption ability of the new adsorbents, and other anions can not compete with phosphate for the active sites of molybdate clusters. As compared to several reported metal oxide-based nanocomposite adsorbents for phosphate removal, FM-201 exhibited great competiveness in terms of selectivity.

The regeneration performance of adsorbents is important considerations for practical applications. Figs. 2c and d show the results of the reusability of FM-201 in five cycles of adsorption-regeneration. Adsorption performance of regenerated FM-201 after acid solution treatment is significantly better than FM-201 regenerated by NaOH solution, despite whether the competitive anions exist or not. Without or with the coexistence of sulphate, the adsorption capacity maintained more than 94.0% or 82.4% of the original value after the 5th cycle respectively. During any cycle, the HCl solution can remove more than 90% of the phosphate captured in the adsorbents (Fig. S7a in Supporting information). After two hours, the desorption process is completed (Fig. S7b in Supporting information). Mo loss from FM-201 is also examined (Table S4 in Supporting information). Mo in FM-201 regenerated by HCl reduced very slightly from 15.74 wt% to 12.69 wt% after 5 cycles, which should be the reason for maintaining the selective adsorption capacity.

To explore the mechanism of phosphate adsorption by FM-201, we performed XPS on FM-201 before and after phosphate adsorption. O 1s spectra of adsorbents are fitted with three speaks, including oxide oxygen (-O-), hydroxyl group bonded to metal (-OH) and adsorbed water (H_2O) (Fig. 3a) [30]. The fitting parameters are reported in Table S5 (Supporting information), it shows that the -OH percentage of initial adsorbent is 65.02%, and great numbers of -OH on the FM-201 surface. And the -OH percentage is remarkably decreased to 31.79% and the -O- percentage is increased to 45.15% after adsorption process due to the phosphate and MoO_x clusters formed the molybdate-phosphate complexes (PO_4•MoO_x) with Mo-O-P bonds.

To figure out the change of interactions between molybdate and phosphate during regeneration, FT-IR (Fig. 3b and Fig. S8 in Supporting information) and Raman spectroscopy (Fig. 3c) are performed. It has been reported MoO_x structures change by the pH of the solution. The used adsorbent is regenerated with HCl solution and NaOH solution respectively, and the IR of regenerated adsorbents are compared with each other. In Fig. 3b, there is no peak at 900–950 cm^{-1} after the adsorbent is desorbed by NaOH solution, the stretching vibration of the molybdate component disappeared.Moreover, The remaining peak at 824 cm^{-1} (Fe-O) in the solid beads indicate that $Fe(OH)_3$ appeared and the clusters of Fe-(MoO_x) disappear in alkaline solution. In Fig. S8 (Supporting information), the adsorption of phosphate produced a negative shift in the stretching vibration of the molybdate component (Mo = O) from 914 and 947 cm^{-1} to 899 and 923 cm^{-1} respectively, resulting from the molybdate-phosphate complexes ($PO_4\cdot MoO_x$). After desorption, the stretching vibration peaks of

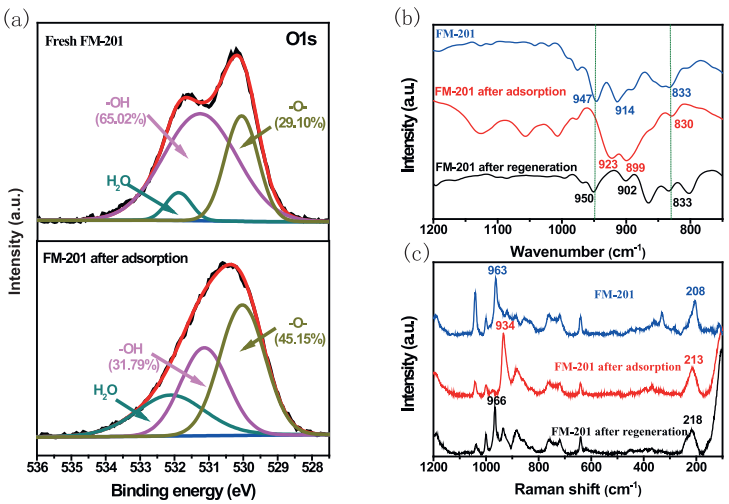

Fig. 3. (a) O 1s XPS spectra of FM-201 before and after phosphate adsorption (adsorbent dose: 0.5 g/L; initial phosphate concentration: 30 mg/L; pH 5; 25 °C; 24 h). (b) FT-IR of FM-201 and FM-201 regenerated by HCl or NaOH solution. (c) Raman spectra of FM-201, FM-201 after adsorption of phosphate and regenerated by HCl solution.

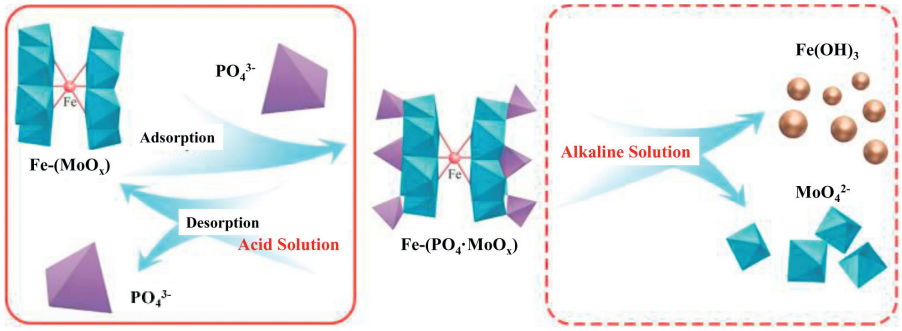

Fig. 4. Schematic illustration of desorption mechanism.

molybdate moved back to the original position. Those prove that the structure of molybdate clusters after regeneration by acid solution are the same as that of the original molybdate clusters. The peak at 833 cm^{-1} indicate the presence of the molybdate group (Mo-O-Fe) for FM-201 (Fig. S8), which did not shift during the adsorption-regeneration cycles.

Raman spectras of molybdate at various pH values and the corresponding ionic species are presented in the report previously (Table S7 in Supporting information) [31]. As the solution pH value is low, the corresponding species of molybdate clusters are $[Mo_8O_{26}]^{4-}$. The support resin D-201 can still firmly fix the clusters $[Mo_8O_{26}]^{4-}$ in the acid solution. However, as the solution pH value is high, the corresponding species of molybdate are $[MoO_4]^{-}$. After regeneration of alkaline solution, molybdate $[MoO_4]^{-}$ in D-201 channels is rapidly lost, which led to a significant decrease in the selective adsorption capacity of the regenerated adsorbent for phosphate. When FM-201 is obtained in ferric nitrate solution, the Raman band of molybdate is 963 cm^{-1}. New Raman band appearing at 934 cm^{-1} after adsorption suggest the presence of a new complexes (PO_4•MoO_x). After regenerated by HCl solution, the Raman band of molybdate moved back to 966 cm^{-1}, this also shows that adsorbent can be well regenerated in acid solution and can be recycled effectively.

As shown in Fig. 4, the interaction mode between molybdate complexes and phosphate in the process of adsorption - regeneration is briefly described. Firstly, due to the chemisorption, only phosphate in the solution (pH 4–8) can be complexed with molybdate Fe-(MoO_x), and the new complexes Fe-(PO_4•MoO_x) appeard. Then FM-201 is desorbed by alkaline solution, $[MoO_4]^{-}$ almost completely escaped, Fe^{3+} is transformed to $Fe(OH)_3$, and the adsorbent is completely damaged. Therefore, FM-201 is only regenerated in acid solution, it is stable and MoO_x is firmly fixed. Fe-(PO_4•MoO_x) is transformed to Fe-(MoO_x). The XPS, FT-IR, and Raman methods are in agreement and reveal their structures transformation.

Combined above research, the simulated wastewater solution is used to test the applicability of FM-201 in a more widely used operation mode (the fixed-bed adsorption runs) [32]. Fig. S9 (Supporting information) illustrates an effluent history of a separate fixed-bed column packed with FM-201 for a solution containing phosphate and other commonly occurring anions (Cl^{-}, SO_4^{2-}, NO_3^{-}, HCO_3^{-}). When the breakthrough point is set as 0.5 mg P/L (the national wastewater discharge standard of China), the effective treatment volume of FM-201 is 4600 BV, whereas that of D-201 is only 300 BV. In addition, FM-201 can even bring down phosphate concentration from 2.5 mg/L to 0.01 mg/L, which further demonstrates the preferable removal of phosphate by the composite adsorbent. The exhausted FM-201 column is then subjected to *in situ* regeneration by 0.1 mol/L HCl (1BV) and 50 g/L $(NH_4)_6Mo_7O_{24}$ (1BV) solution successively at room temperature. Prior to the next run, the FM-201 column is rinsed with deionized water until the effluent pH is neutral.

In this study, we employed a new adsorbent FM-201, which has excellent selective and durable phosphate removal ability. Molybdate complexes act as the core active species because of the controlled complexation with phosphate. We put forward the new method which related to regeneration of adsorbent by molybdate

complexes structures transformation in acid solution. This work may provide new insight into the design of the promising adsorbents for highly selective removal of phosphate.

Declaration of competing interest

The authors declare that they have no known competing financial interests or personal relationships that could have appeared to influence the work reported in this paper.

Acknowledgments

This study was supported by the National Natural Science Foundation of China (Nos. 52070100, 51978341), the Natural Science Foundation of Jiangsu Province of China (No. BK20190087).

Supplementary materials

Supplementary material associated with this article can be found, in the online version, at doi:10.1016/j.cclet.2021.04.027.

References

[1] D.W. Schindler, S.R. Carpenter, S.C. Chapra, R.E. Hecky, Environ. Sci. Technol. 50 (2016) 8923–8929.
[2] B. Wu, J. Wan, Y.Y. Zhang, B.C. Pan, I.M.C. Lo, Environ. Sci. Technol. 54 (2020) 50–66.
[3] Q.R. Zhang, J. Teng, G.D. Zou, et al., Nanoscale 8 (2016) 7085–7093.
[4] X. Ge, X.Y. Song, Y. Ma, et al., J. Mater Chem. A 4 (2016) 14814–14826.
[5] M. Kunaschk, V. Schmalz, N. Dietrich, T. Dittmar, E. Worch, Water Res. 71 (2015) 219–226.
[6] Y.Y. Zhang, B.C. Pan, C. Shan, X. Gao, Environ. Sci. Technol. 50 (2016) 1447–1454.
[7] P.J.J. Alvarez, C.K. Chan, M. Elimelech, N.J. Halas, D. Villagrán, Nat. Nanotechnol. 13 (2018) 634–641.
[8] E.M. Zong, G.B. Huang, X.H. Liu, et al., J. Mater Chem. A 6 (2018) 9971–9983.
[9] J.A. O'Neal, T.H. Boyer, Water Res. 47 (2013) 5003–5017.
[10] S. Sengupta, A. Pandit, Water Res. 45 (2011) 3318–3330.
[11] Y. Su, H. Cui, Q. Li, S.A. Gao, J.K. Shang, Water Res. 47 (2013) 5018–5026.
[12] N.Y. Acelas, B.D. Martin, D. López, B. Jefferson, Chemosphere 119 (2015) 1353–1360.
[13] R.H. Li, J.J. Wang, Z.Q. Zhang, et al., Sci. Total Environ. 11 (2018) 526–536.
[14] B.L. Wu, I.M.C. Lo, Environ. Sci. Technol. 54 (2020) 4601–4608.
[15] L. Chen, X. Zhao, B.C. Pan, et al., J. Hazard. Mater. 284 (2015) 35–42.
[16] A. Sjösten, S. Blomqvist. Water Res. 31 (1997) 1818–1823.
[17] Z.A. Othman, Inamuddin Naushad M., Chem. Eng. J. 166 (2011) 639–645.
[18] R.R. Sheha, S.H.E. Khouly, Chem. Eng. Res. Des. 91 (2013) 942–954.
[19] H. Zhu, X. Yang, E.D. Cranston, S.P. Zhu, Adv. Mater. 28 (2016) 7652–7657.
[20] D. Pang, C.C. Wang, P. Wang, et al., Chemosphere 254 (2020) 126829.
[21] J. Xie, D.Fang Z.Wang, C.J. Li, D.Y. Wu, J. Colloid Interface Sci. 423 (2014) 13–19.
[22] R.S.S. Wu, K.H. Lam, J.M.N. Lee, T.C. Lau, Chemosphere 69 (2007) 289–294.
[23] C. Anthony, P. Wersin. Environ. Sci. Technol. 41 (2007) 5002–5007.
[24] J.S. Qian, X. Gao, B.C. Pan, Environ. Sci. Technol. 54 (2020) 8509–8526.
[25] S. Sarkar, A.K. SenGupta, P. Prakash, Environ. Sci. Technol. 44 (2010) 1161–1166.
[26] T.H. Bui, S.P. Hong, J. Yoon, Water Res. 134 (2018) 22–31.
[27] H. Oudghiri-Hassani, Catal. Commun. 60 (2015) 19–22.
[28] N.Y. Mezenner, A. Bensmaili, Chem. Eng. J. 147 (2009) 87–96.
[29] B.J. Pan, J. Wu, B.C. Pan, et al., Water Res. 43 (2009) 4421–4429.
[30] M. Mallet, K. Barthelemy, C. Ruby, A. Renard, S. Naille, J. Colloid Interface Sci. 407 (2013) 95–101.
[31] H.J. Tian, C.A. Roberts, I.E. Wachs, J. Phys. Chem. C 114 (2010) 14110–14120.
[32] M. Hua, L.L. Xiao, B.C. Pan, Q.X. Zhang, Front. Environ. Sci. Eng. 7 (2013) 435–441.